

# Quantifying Axonal Responses in Patient-Specific Models of Subthalamic Deep Brain Stimulation

Kabilar Gunalan\*, Bryan Howell\*, Cameron C. McIntyre

Department of Biomedical Engineering, Case Western Reserve University, Cleveland, Ohio, USA

\*K. Gunalan and B. Howell contributed equally to this work

---

## Supplementary methods

### A. Weights for DF-Peterson

For a given stimulus pulse width (PW) and axon diameter ( $D$ ), weights are calculated by applying a monophasic intracellular point-source stimulus that is PW in duration to a node of Ranvier (NoR). At a reference NoR, the maximum transmembrane voltage (i.e. the maximum  $V_{m,0}$ ) reached during or after stimulation is calculated. The middle NoR of a long cable is typically designated as the reference NoR, which in the above description (see ‘DF-Peterson’), corresponds to  $i = 0$ . The process is then repeated by applying the intracellular stimulus, one at a time, to all other NoR.  $w_i$  is the maximum  $V_{m,0}$  observed over time when the stimulus is applied at the  $i^{\text{th}}$  NoR divided by the same quantity but when the stimulus is applied to the reference NoR at  $i = 0$ .  $w_0$  is thereby 1, and all other  $w_i$  are between 0 and 1. For more details on the motivation behind this type of weighting, we refer the reader to the work by Warman et al. [1992].

## B. Bilinear interpolation

We used bilinear interpolation to approximate parameters and values used in DF-Peterson and VTA-Astrom at combinations of D and PW not reported in the respective works. In DF-Peterson, we are referring to the weights,  $\Phi_{e,0,th}$ , and  $MDF_{th}$ ; and in VTA-Astrom, we are referring to  $E_{T,th}$  (Figure S2). To approximate the dependent variable of interest,  $y^*$ , we applied the following matrix formula:

$$y^* = [1 \quad D^* \quad PW^* \quad D^*PW^*] \begin{bmatrix} 1 & D_1 & PW_1 & D_1PW_1 \\ 1 & D_1 & PW_2 & D_1PW_2 \\ 1 & D_2 & PW_1 & D_2PW_1 \\ 1 & D_2 & PW_2 & D_2PW_2 \end{bmatrix}^{-1} \begin{bmatrix} y_{11} \\ y_{12} \\ y_{21} \\ y_{22} \end{bmatrix} \quad (S1)$$

, where  $D^*$  and  $PW^*$  are the respective independent variables.  $D_1$  and  $D_2$  are the closest values (inclusive) below and above  $D^*$ , respectively;  $PW_1$  and  $PW_2$  are the closest values (inclusive) above and below  $PW^*$ , respectively; and  $y_{ij}$  is the respective value at  $D_i$  and  $PW_j$ , for  $i,j = 1,2$ . Note, multiplication of the latter two matrices in Equation S1 yields the coefficients for bilinear interpolation.

## C. Activation volume tractography

Activation volume tractography (AVT) was performed by calculating those streamlines that originated from the VTA-Chaturvedi ellipsoid and terminated in the ventral lateral posteroventral (VLpv) thalamic nucleus (Figure 10B). We performed tractography from the voxels with centers within a 1 V VTA-Chaturvedi ellipsoid (Figure 10B2). We used 320 seeds per voxel, which was equivalent to 5,000 seeds per  $mm^3$ . Those streamlines that intersected the VLpv thalamic nucleus and avoided the ipsilateral CSF and contralateral cerebral hemisphere were retained (Figure 10B3). This resulted in a total of 37,163 streamlines, or 16.0% of the streamlines originating from the VTA-Chaturvedi. We repeated this process but also excluded streamlines that passed through the globus pallidus, substantia nigra, ventral lateral anterior (VLa) thalamic nucleus, ventral posterior lateral (VPL) thalamic nucleus, and took a trajectory above the VLpv thalamic nucleus, totaling 7 exclusion criteria. This resulted in 31,911 streamlines, or 13.7% (Figure 10B4). We also performed tractography for a 2 V VTA-Chaturvedi ellipsoid with all 7 exclusion criteria, which totaled 52,450 streamlines or 15.1% (Figure 10B5).





## Supplementary figures

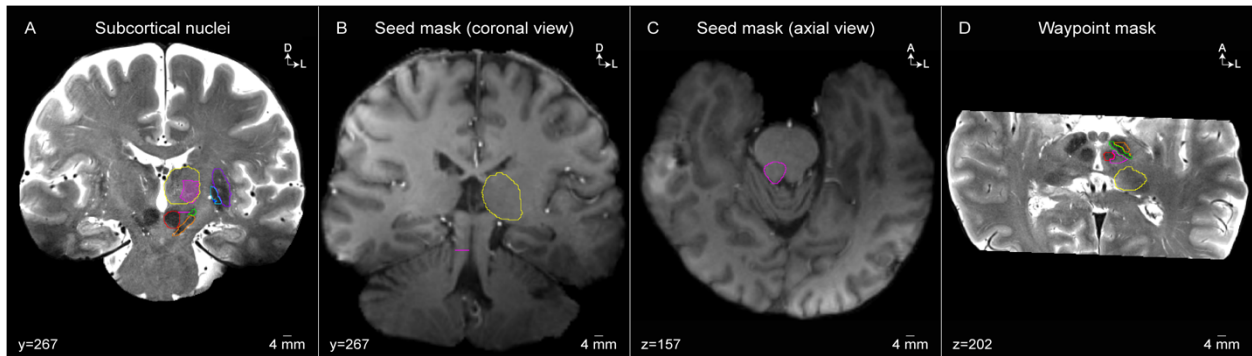


**Figure S1.** Masks for constructing the cerebellothalamic tract with tractography. (A) Coronal view of subcortical nuclei overlaid on the 7T T2-weighted (T2W) image (subthalamic nucleus—green, substantia nigra—orange, red nucleus—red, thalamus—yellow, ventral lateral posteroventral thalamic nucleus—striped pink, putamen—purple, globus pallidus externus—light blue, globus pallidus internus—dark blue). The pink line indicates the waypoint mask shown in D. (B) Coronal view of the seed mask in the superior cerebellar peduncle (pink) overlaid on the 7T T1-weighted (T1W) image. (C) Axial view of the seed mask in the superior cerebellar peduncle (pink) overlaid on the 7T T1W image. (D) Axial view of the waypoint mask between the subthalamic nucleus and red nucleus overlaid on the 7T T2W image.

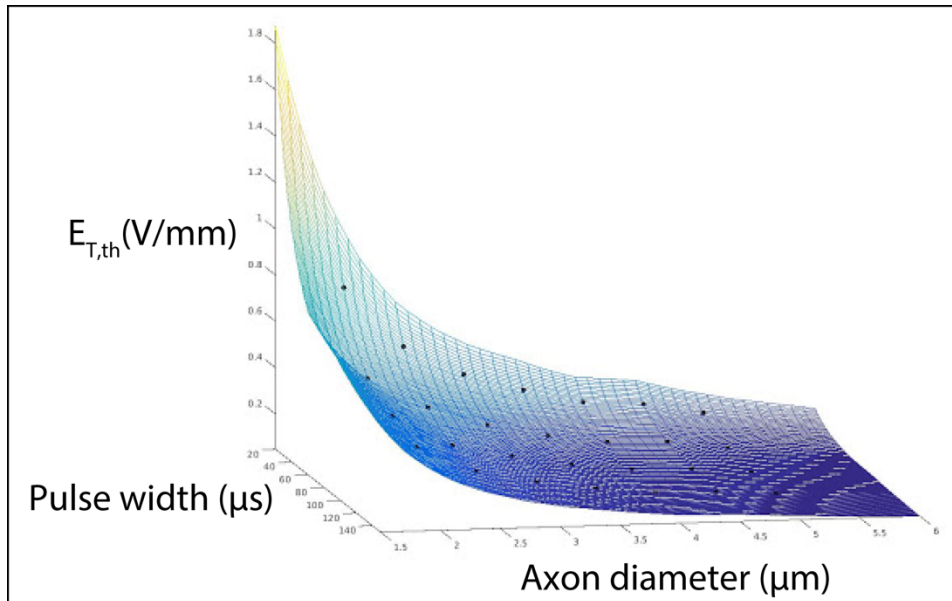


**Figure S2.** VTA-Astrom electric field strength threshold values ( $E_{T,th}$ ). We used bilinear interpolation of the reported values (black dots) to create a continuous function.

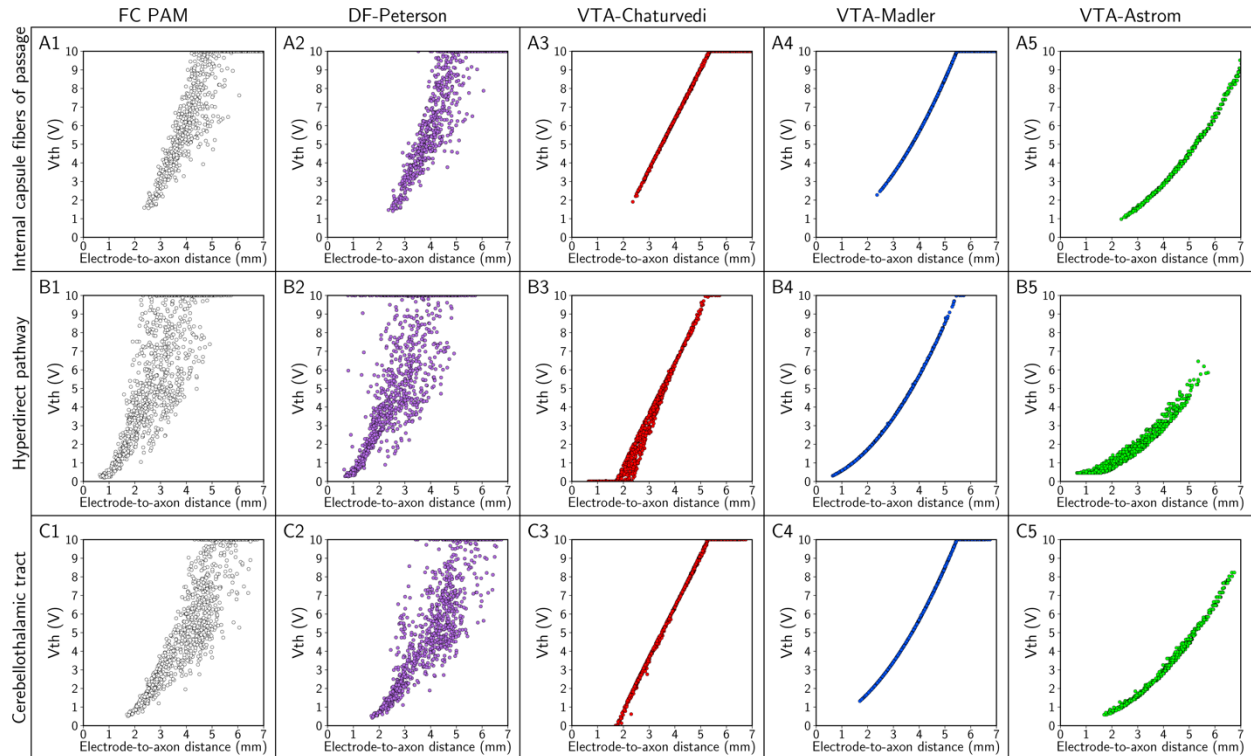


**Figure S3.** Strength-distance relationship of the threshold stimulus amplitudes ( $V_{th}$ ) for action potential initiation calculated with the FC, DF, and VTA PAMs. Thresholds were calculated for the: (A) internal capsule fibers of passage, (B) hyperdirect pathway, and (C) cerebellothalamic tract. The stimulus pulse width was  $90 \mu\text{s}$ , electrode configuration was contact 2 (-), case (+), and axon diameter was  $5.7 \mu\text{m}$ . In this plot, we set axons with  $V_{th} > 10 \text{ V}$  as  $10 \text{ V}$ , so that all axons representing a pathway can be visualized in the field of view. Note, electrode-to-axon distance is calculated from the center of the electrode contact.

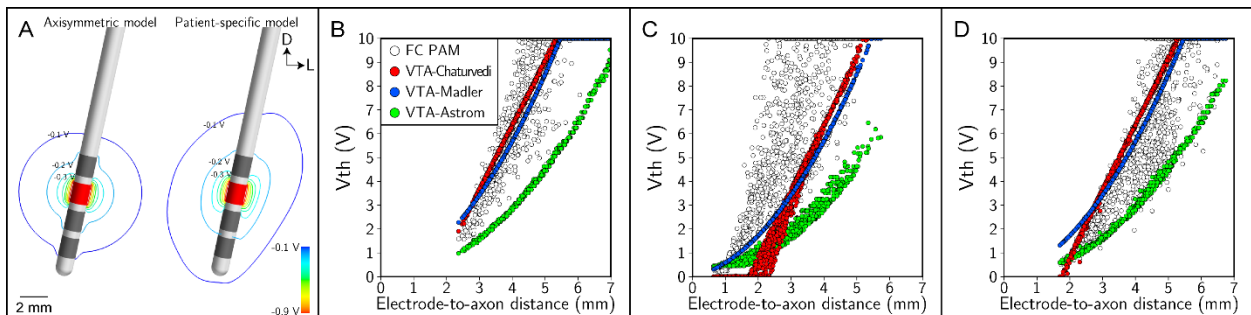


**Figure S3 overlay.** Strength-distance relationships. (A) Isopotential contours for a  $-1 \text{ V}$  stimulus amplitude created with (left) an axisymmetric model aligned to the trajectory of the patient-specific electrode and (right) the patient-specific model. (B-D) Strength-distance relationships. Thresholds were calculated for the: (B) internal capsule fibers of passage, (C) hyperdirect pathway, and (D) cerebellothalamic tract. The stimulus pulse width was  $90 \mu\text{s}$ , electrode configuration was contact 2 (-), case (+), and axon diameter was  $5.7 \mu\text{m}$ . In this plot, we set axons with  $V_{th} > 10 \text{ V}$  as  $10 \text{ V}$ , so that all axons representing a pathway can be visualized in the field of view. Note, electrode-to-axon distance is calculated from the center of the electrode contact.

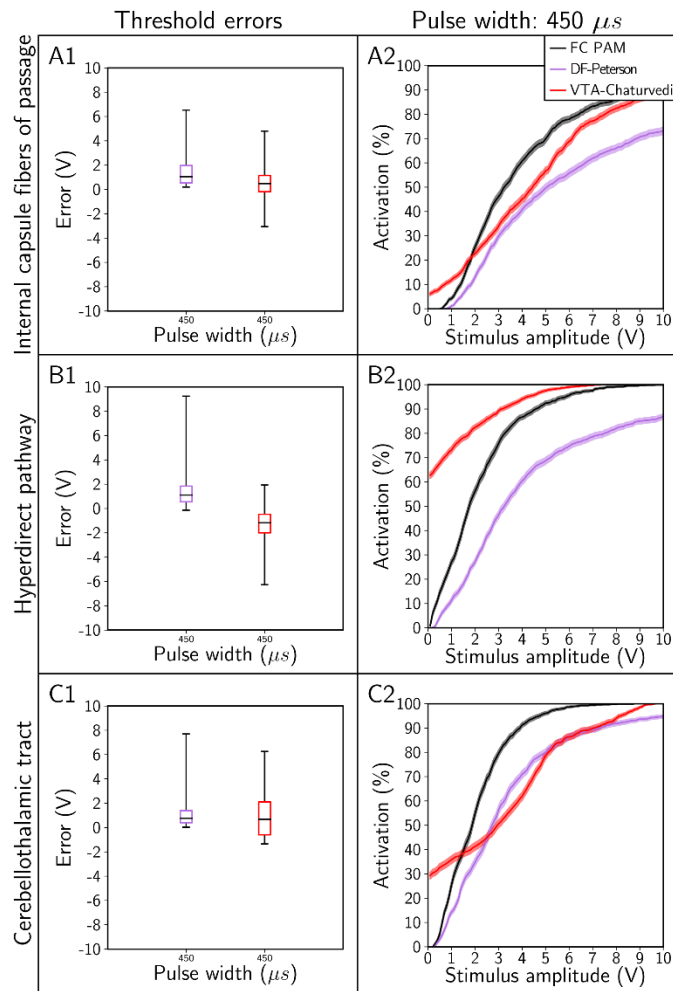


**Figure S4.** Errors in stimulation thresholds and recruitment curves generated with the FC, DF, and VTA PAMs using a pulse width of 450  $\mu s$ . Recruitment curves were calculated for the: (A) internal capsule fibers of passage, (B) hyperdirect pathway, and (C) cerebellothalamic tract. The electrode configuration was contact 2 (-), case (+) and axon diameter was 5.7  $\mu m$ .

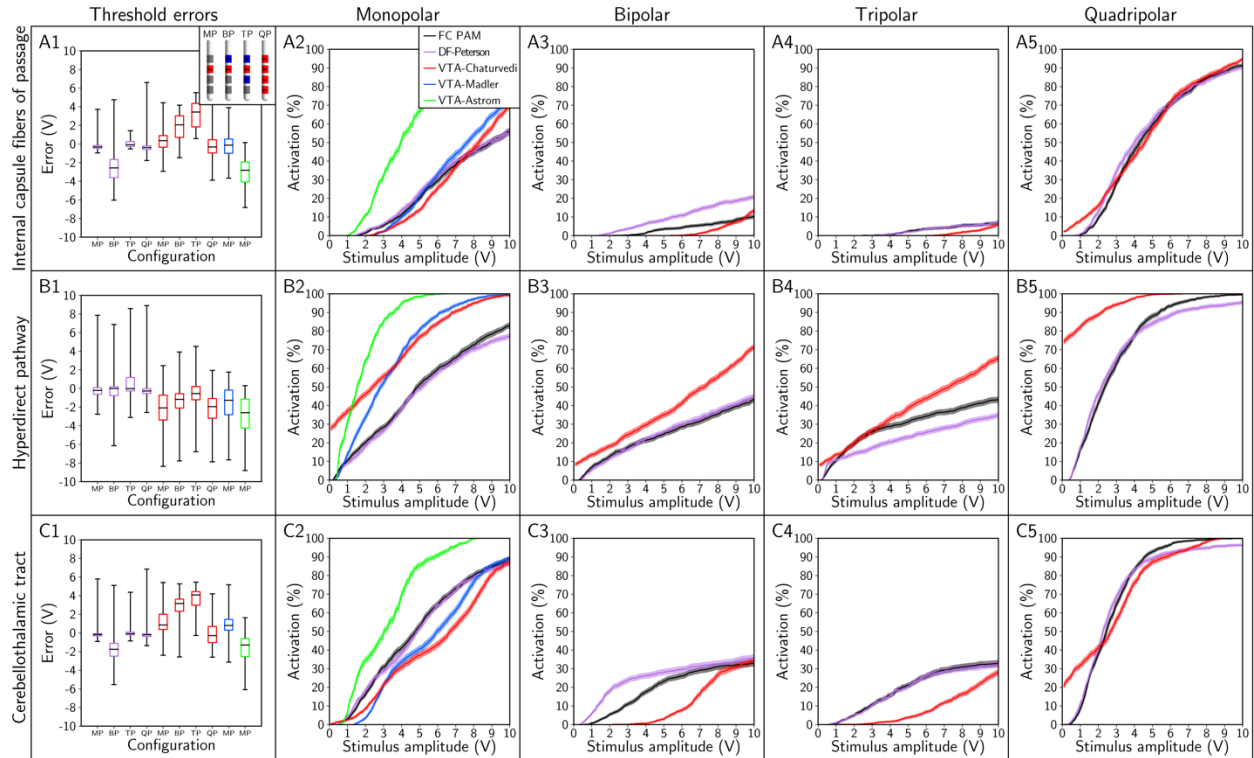


**Figure S5.** Errors in stimulation thresholds and recruitment curves generated with the FC, DF, and VTA PAMs for electrode configurations of monopolar (MP; contact 2 [-], case [+]), bipolar (BP; contact 2 [-], contact 3 [+]), tripolar (TP; contact 1 [+], contact 2 [-], contact 3 [+]), and quadripolar (QP; contact 0 [-], contact 1 [-], contact 2 [-], contact 3 [-], case [+]). Recruitment curves were calculated for the: (A) internal capsule fibers of passage, (B) hyperdirect pathway, and (C) cerebellothalamic tract. The stimulus pulse width was 90  $\mu$ s and axon diameter was 5.7  $\mu$ m.



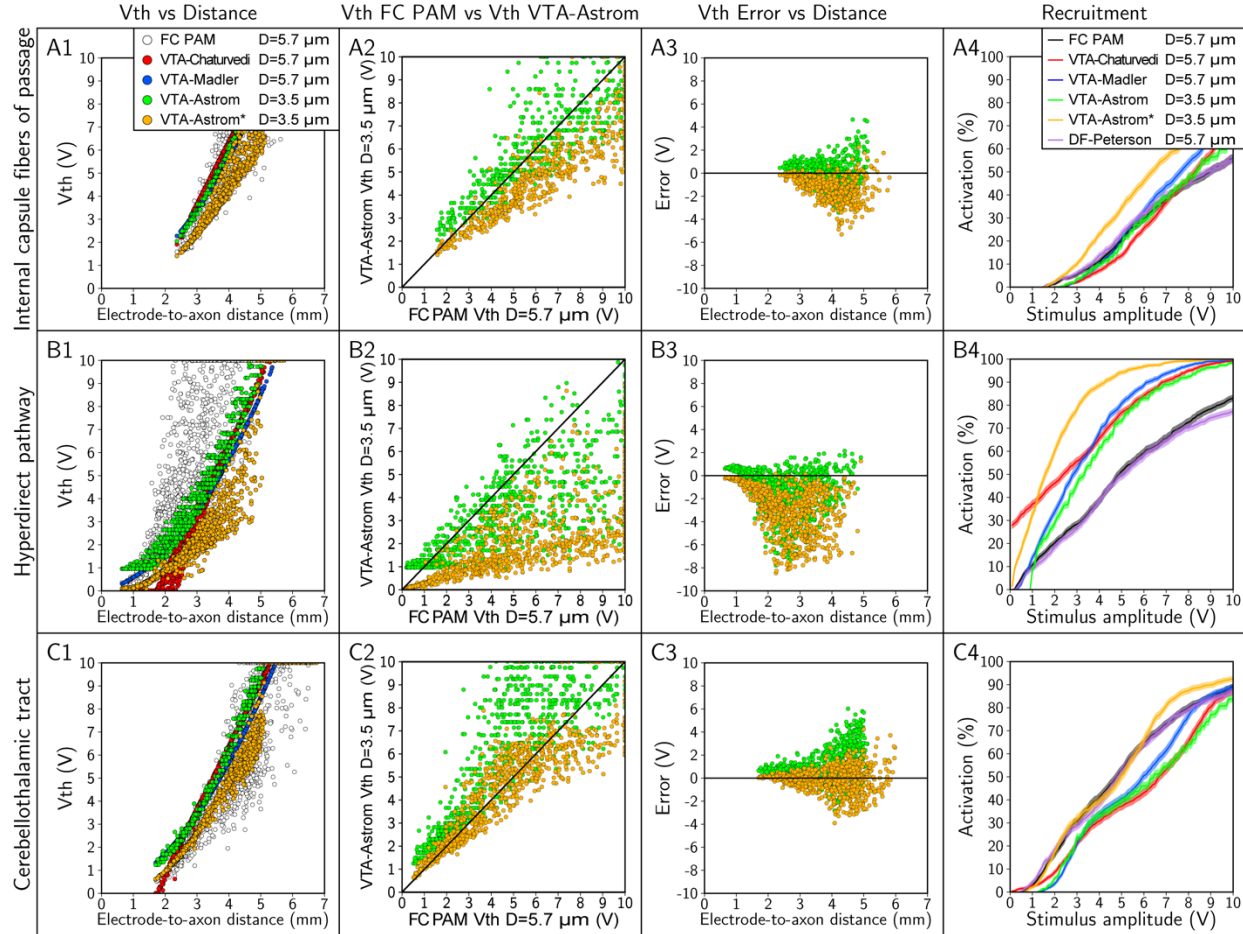


**Figure S6.** Results for the VTA PAM developed by Astrom et al. [2015] for an axon diameter ( $D$ ) of  $3.5 \mu\text{m}$ . The VTA-Astrom results were calculated with an isotropic, homogeneous volume conductor model and VTA-Astrom\* results were calculated with the patient-specific volume conductor model. The FC, DF-Peterson, VTA-Chaturvedi, and VTA-Madler PAMs were calculated for  $D=5.7 \mu\text{m}$ . The rows denote results for the: (A) internal capsule fibers of passage, (B) hyperdirect pathway, and (C) cerebellothalamic tract. (1) Threshold stimulus amplitude ( $V_{\text{th}}$ ) as a function of electrode-to-axon distance. In this plot, we set axons with  $V_{\text{th}} > 10 \text{ V}$  as  $10 \text{ V}$ , so that all axons representing a pathway can be visualized in the field of view. Electrode-to-axon distance is calculated from the center of the electrode contact. (2)  $V_{\text{th}}$  of the VTA-Astrom ( $D=3.5 \mu\text{m}$ ) and VTA-Astrom\* ( $D=3.5 \mu\text{m}$ ) as a function of the  $V_{\text{th}}$  of the FC PAM ( $D=5.7 \mu\text{m}$ ). In this plot, we set axons with  $V_{\text{th}} > 10 \text{ V}$  as  $10 \text{ V}$ , so that all axons representing a pathway can be visualized in the field of view. (3) Errors in the  $V_{\text{th}}$  of the VTA-Astrom ( $D=3.5 \mu\text{m}$ ) and VTA-Astrom\* ( $D=3.5 \mu\text{m}$ ) as a function of electrode-to-axon distance. (4) Recruitment curves calculated with each method. The stimulus pulse width was  $90 \mu\text{s}$  and electrode configuration was contact 2 (-), case (+).

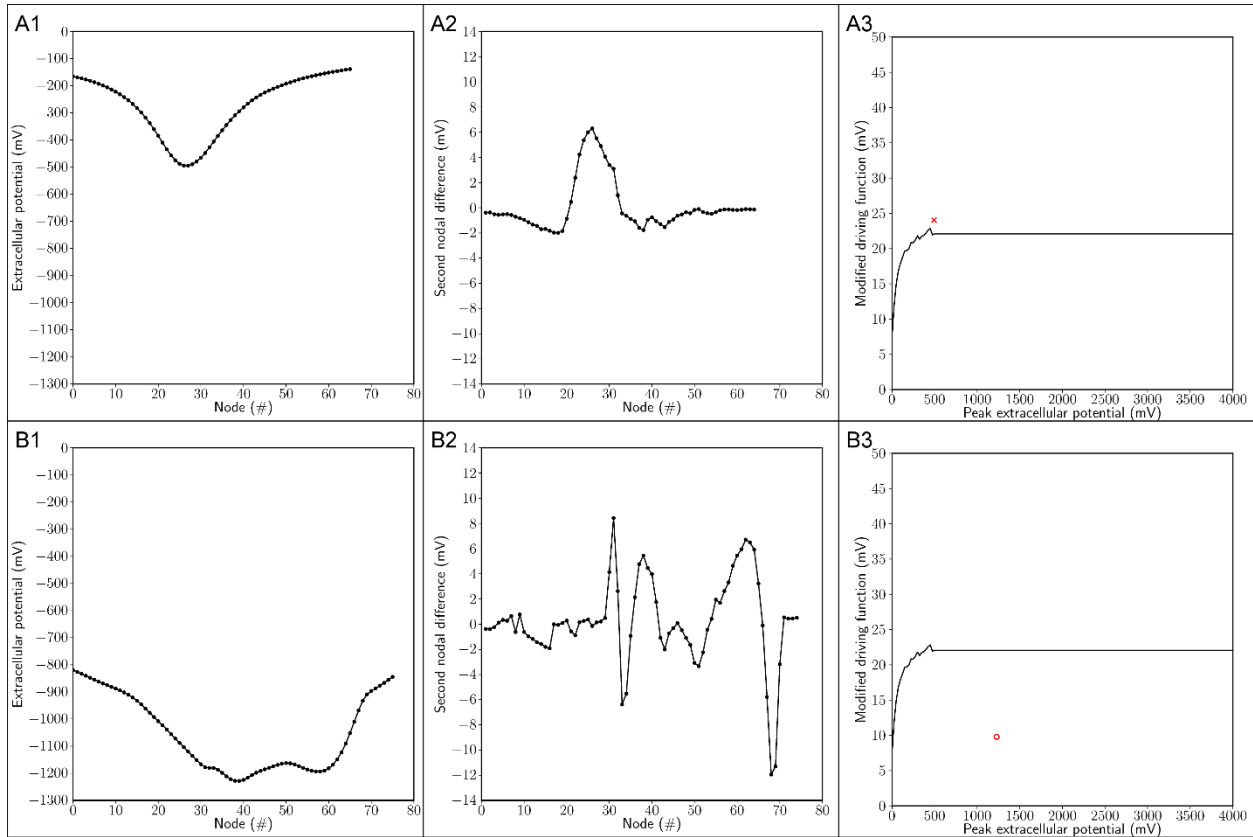


**Figure S7.** Effect of second differences of the extracellular potentials in a patient-specific volume conductor on the modified driving force (MDF) calculation as defined by Peterson et al. [2011]. (A) Internal capsule axon with a FC PAM threshold stimulus amplitude ( $V_{th}$ ) of 3.45 V and DF-Peterson  $V_{th}$  of 3.23 V. (B) Internal capsule axon with a FC PAM  $V_{th}$  of 20.83 V and DF-Peterson  $V_{th}$  of 47.0 V. (A1/B1) Extracellular potentials at the nodes of Ranvier. (A2/B2) Second differences of the extracellular potentials at the nodes of Ranvier. (A3/B3) MDF calculation at the FC PAM  $V_{th}$ . Peterson et al. [2011] threshold modified driving force ( $MDF_{th}$ ) values as a function of the maximum extracellular potential (black line). Patient-specific axons with a  $MDF_{th}$  that lie above the threshold curve are classified as active (red cross) by the DF-Peterson predictor, and those that lie below the threshold curve are classified as not active (red circle). All data is shown at the threshold amplitude for action potential initiation as determined by the FC PAM. The stimulus pulse width was 90  $\mu$ s, electrode configuration was contact 2 (-), case (+), and axon diameter was 5.7  $\mu$ m.

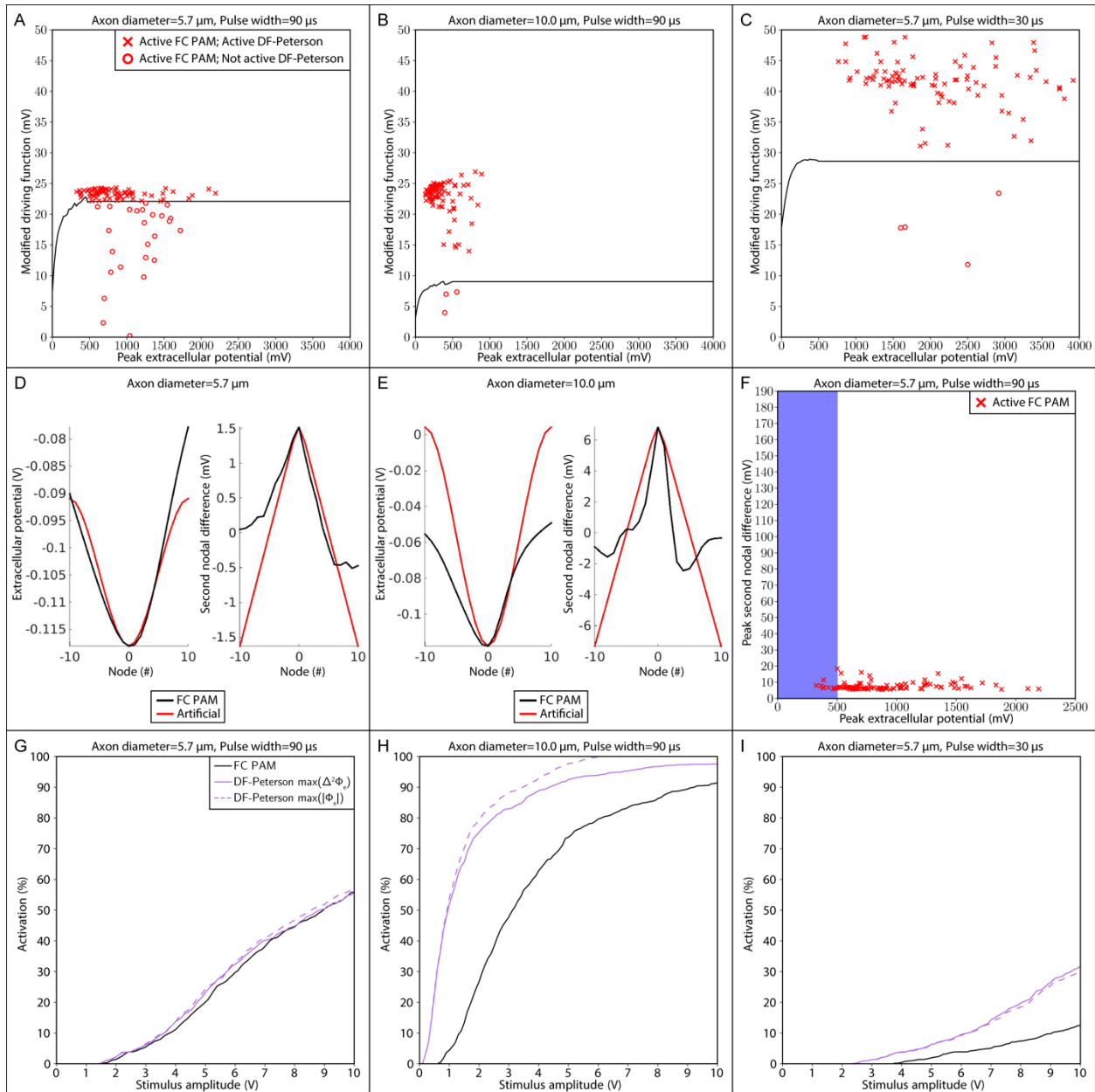


**Figure S8.** Effect of axon diameter and stimulus pulse width on modified driving force (MDF) calculation as defined by Peterson et al. [2011]. (A-C) MDF values at the threshold amplitude for action potential initiation as calculated by the FC PAM. If the MDF value is above the threshold MDF curve ( $MDF_{th}$ , black line) the axon is defined as active (red cross) by the DF-Peterson predictor and if the axon is below the  $MDF_{th}$  curve the axon is defined as not active (red circle). Data is presented for the (A) axon diameter of  $5.7 \mu\text{m}$  and stimulus pulse width of  $90 \mu\text{s}$ , (B) axon diameter of  $10.0 \mu\text{m}$  and stimulus pulse width of  $90 \mu\text{s}$ , and (C) axon diameter of  $5.7 \mu\text{m}$  and stimulus pulse width of  $30 \mu\text{s}$ . (D-E) Extracellular potentials and second differences of the extracellular potentials for the same axon with a diameter of either (D)  $5.7 \mu\text{m}$  or (E)  $10.0 \mu\text{m}$ . Extracellular potentials were developed by Peterson et al. [2011] for their training data set (red, ‘Artificial’) or from the patient-specific volume conductor model (black, ‘FC PAM’). (F) Peak extracellular potentials and second nodal differences at the threshold amplitude for action potential initiation as calculated by the FC PAM of 100 internal capsule axons. The parameter

space that Peterson et al. [2011] developed their training data set (blue box). (G-I) Recruitment curves for activation of the internal capsule as calculated by the FC PAM (solid black line), DF-Peterson predictor using the maximum second nodal difference of the extracellular potentials ( $\Delta^2\Phi_e$ ) to define node 0 for the MDF calculation (solid purple line), or DF-Peterson predictor using the maximum absolute value of the extracellular potentials ( $|\Phi_e|$ ) to define node 0 (dashed purple line).